A New Sequencing Control Strategy for Air-Handling Units

John E. Seem, Ph.D.
Member ASHRAE

Cheol Park, Ph.D.

John M. House, Ph.D.
Assoc. Member ASHRAE

Air-handling unit (AHU) controllers commonly use sequencing logic to determine the most economic way to use the components of the AHU to maintain the supply air temperature at a setpoint value. The objective of this paper is to introduce the finite state machine (FSM) sequencing control strategy for AHUs and to compare this strategy with a traditional split-range sequencing control strategy. The FSM control strategy represents a paradigm shift in the way sequencing logic is developed, illustrated, and implemented for the control of HVAC systems. Simulation results obtained from representative weather data for each month of the year are presented to demonstrate the performance of the two sequencing strategies with respect to the controller gains (proportional gain and integral time) used for the heating coil, cooling coil, and mixing box dampers. Simulation results demonstrate that in comparison to the split-range control strategy, the FSM control strategy leads to more stable operation of the AHU when the feedback controller(s) used to control the supply air temperature is (are) poorly tuned.

INTRODUCTION

One of the primary purposes of an air-handling unit (AHU) is to distribute conditioned air to the occupied zones of a building. The supply air to a particular zone must offset the thermal loads imposed on that zone in order to maintain a comfortable environment for occupants. Because thermal loads for the zones can vary markedly, it is common for an AHU to be controlled to maintain the supply air temperature at a setpoint value that is sufficiently low to satisfy the zone with the largest cooling load at any given time. If needed, the air stream can be throttled and/or reheated at terminal boxes to provide adequate comfort in all zones.

AHU controllers commonly use sequencing logic to determine the most economic use of the components of the AHU to maintain the supply air temperature at the setpoint value. For instance, it is not uncommon for a building subjected to large daily temperature swings to require heating in the morning and mechanical cooling in the afternoon. Costs associated with mechanical cooling can be reduced using economizer cycle control. Economizer cycle control involves modulating dampers located in the mixing box to control the amount of outdoor air introduced to the AHU. Under certain outdoor air conditions, the supply air temperature can be maintained at the setpoint value without the use (or with reduced use) of mechanical cooling. When the AHU is operating in the mechanical cooling mode, the outdoor air damper is either fully open or it is set to a minimum position. Economizer cycle control logic includes a comparison of the outdoor and return air temperatures or enthalpies to determine the proper position of the outdoor air damper for this situation. If the outdoor air temperature (enthalpy) is greater than some minimum value and less than the return air temperature (enthalpy), an opportunity exists to reduce mechanical cooling costs by

John E. Seem is a principal research engineer at Johnson Controls, Inc., Milwaukee, WI. **Cheol Park** and **John M. House** are mechanical engineers in the Mechanical Systems and Controls Group, Building Environment Division, Building and Fire Research Laboratory, National Institute of Standards and Technology, Gaithersburg, MD.

using 100% outdoor air in the AHU. Sequencing logic determines the mode of operation of an AHU at any particular time.

Numerous studies related to sequencing logic and economizer cycle control strategies appear in the literature. Spitler et al. (1987) used computer simulations to compare a temperature-based economizer strategy with an enthalpy-based strategy for two buildings in five different cities. Park et al. (1984), Dickson and Tom (1986), and Wang (1993) contain details for implementing economy cycle control strategies.

On the surface, sequencing logic and economizer cycle control are quite intuitive. In practice, however, the logic can be difficult to program and difficult to follow. According to Hartman (1993), the direct digital controls industry has not yet found an effective means to represent system level logic. Despite the advent of digital control systems and considerable effort on the part of the HVAC controls industry, sequencing control problems once common in pneumatic control systems persist today. One such problem is documented in ASHRAE (1995). Results for an actual AHU are presented that show an outdoor air damper and heating coil valve cycling between fully open and fully closed approximately every two minutes. This wastes energy and leads to excessive component wear. The move to digital control has done little to improve the situation because, rather than taking full advantage of the programming capabilities of digital controllers, logic used with pneumatic control systems has simply been transferred to the digital controllers.

The objective of this paper is to introduce a new sequencing control strategy for AHUs and to compare this strategy with a traditional split-range sequencing control strategy. The new strategy is referred to as the finite state machine (FSM) sequencing control strategy. The FSM control strategy represents a paradigm shift in the way sequencing logic is developed, illustrated, and implemented for the control of HVAC systems. The inherent advantages of the FSM control strategy over the split-range control strategy are highlighted in this paper.

The paper is organized in the following manner. First, a description of an AHU and its operation is provided. Next, the split-range and FSM control strategies are presented. Validation exercise results for an artificial outdoor air temperature profile are then presented to demonstrate that the two strategies produce nearly the same results for a limiting case. Additional simulations are performed to determine the most appropriate value of the state transition delay used in the FSM control strategy. Simulation results obtained from representative weather data for each month of the year are then presented to demonstrate the performance of the two sequencing strategies with respect to the controller gains (proportional gain and integral time) used for the heating coil, cooling coil, and mixing box dampers. Finally, conclusions for this study are then presented.

SYSTEM DESCRIPTION

Figure 1 shows a schematic diagram of an AHU. The description of the AHU will be restricted to the components used to maintain the supply air temperature at the setpoint value.

Air enters the AHU through the outdoor air damper and, depending on the mixing box damper settings, may be mixed with air passing through the recirculation air damper. The temperatures and flow rates of the outdoor and recirculation air streams determine the conditions at the exit of the mixed air plenum. Air exiting the mixed air plenum passes through the heating and cooling coils. At most, only one of the two coils will be active at any given time assuming the sequencing control strategy is implemented properly and there are no valve leaks or other faults in the system. After being conditioned in the coils, the air is distributed to the zones through the supply air ductwork. The supply air temperature is measured downstream of the supply fan. Return air is drawn from the zones by the return fan and is either exhausted or recirculated, depending once again on the position of the mixing box dampers. The return air temperature is measured downstream of the return fan.

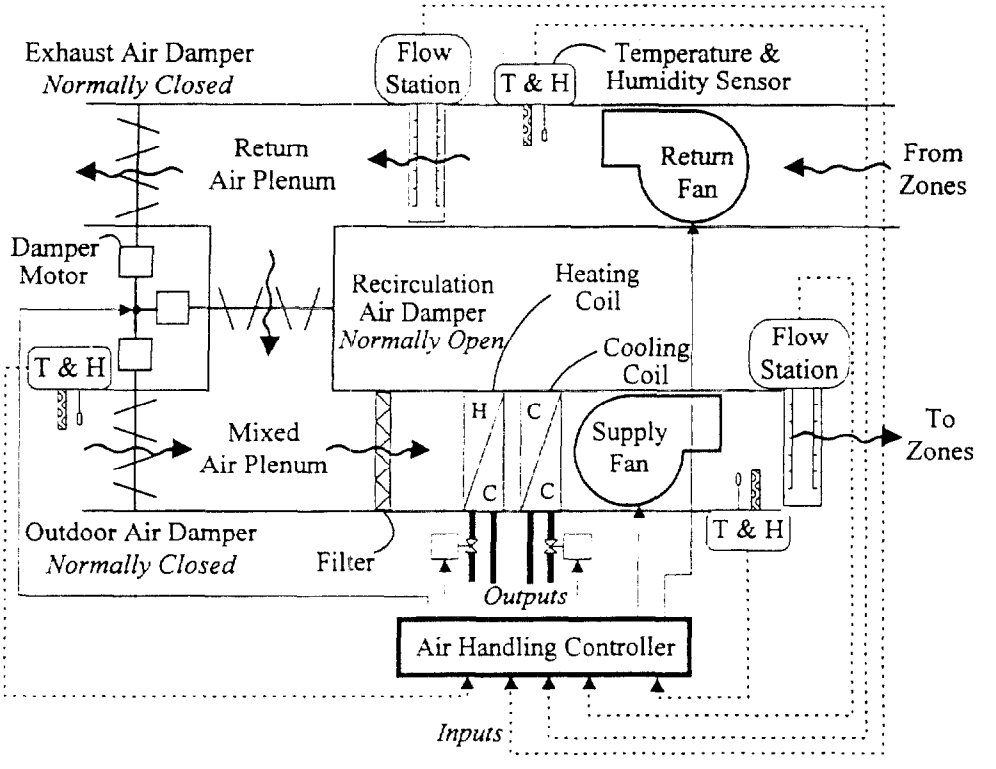

Figure 1. Schematic diagram of an air-handling unit

The air handling controller in Figure 1 includes a feedback controller (or controllers) and sequencing logic. The feedback controller controls the heating coil, the cooling coil, and the mixing box dampers.

SPLIT-RANGE SEQUENCING CONTROL STRATEGY

Figure 2 shows a flow chart for a split-range sequencing control strategy that would be implemented in the air handling controller shown in Figure 1. Split-range control has traditionally been used for HVAC applications in which a single measured variable is used to determine outputs to several controlled devices (Åström and Hägglund 1995, Ogunnaike and Ray 1994). In this study, the measured variable is the supply air temperature and the controlled devices are the cooling coil valve, the heating coil valve, and the mixing box dampers. In traditional pneumatic control systems, a single feedback controller, usually a proportional-integral (PI) controller, was used with this strategy to reduce component costs. The split-range control strategy continues to be popular in today's digital control systems.

Figure 3 shows the relationship between the feedback controller output (u) and the control signal to the valves and dampers for a split-range control strategy applied to an AHU. The controller output is represented with a continuous scale ranging from −100% to 200%. This scale is somewhat arbitrary (a voltage range could also be used) and is selected to emphasize the fact that the outputs to three actuators, each having a control signal corresponding to 0% to 100% open, are determined by a single feedback controller. The controller output is determined by comparing the supply air temperature with its setpoint value. If the output from the feedback controller is between 100% and 200%, mechanical cooling is used to cool the air. Here 100% represents no

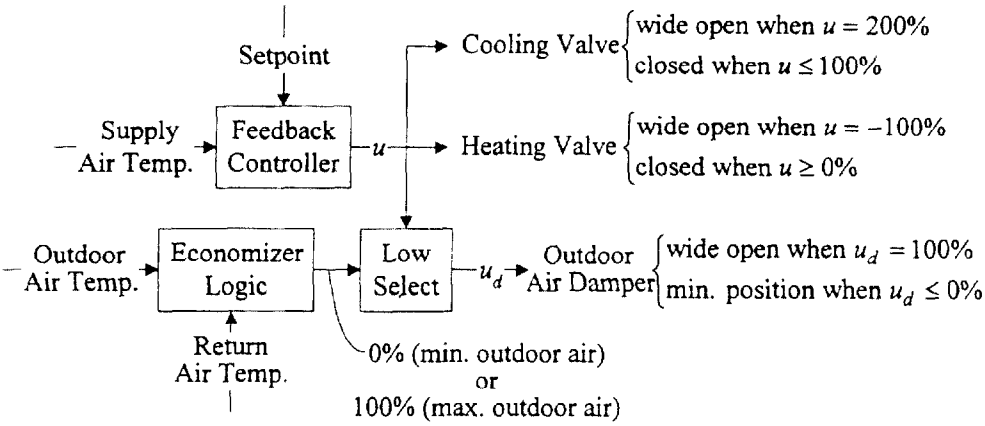

Figure 2. Split-range control strategy for air-handling units

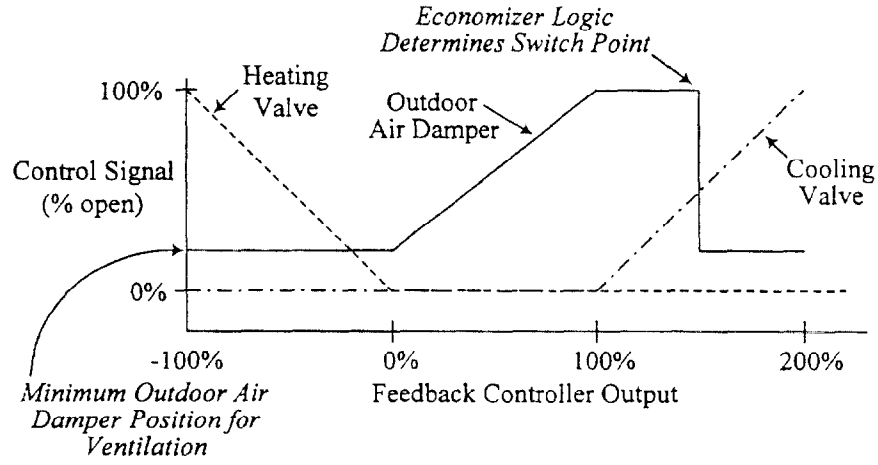

Figure 3. Relationship between split-range controller output and signals to dampers and valves

mechanical cooling and 200% represents maximum mechanical cooling. If the outdoor air conditions are suitable, economizer cycle control (outdoor air dampers fully open) is used simultaneously to reduce the mechanical cooling load. If the output from the feedback controller is between −100% and 0%, the heating coil is used to heat the supply air and the outdoor air damper is at its minimum position determined by ventilation criteria. If the output from the feedback controller is between 0% and 100%, the dampers are modulated to control the amount of outdoor air and return air that are mixed to produce supply air at the setpoint temperature. This is referred to as cooling with outdoor air (also sometimes referred to as free cooling) because mechanical cooling is not used.

The dynamic characteristics of heating, mechanical cooling, and cooling with outdoor air (hereafter referred to as heating, cooling, and cooling with outdoor air) may be significantly different. If this is the case, the use of a single feedback controller may be very limiting because to maintain stable control, the controller gains must be tuned for the worst-case conditions. The

result of this conservative selection of controller tuning parameters is that the closed-loop response for other conditions will tend to be sluggish. If the feedback controller is not tuned for the worst-case conditions, then the valves and mixing box dampers may cycle between fully open and fully closed with resultant energy waste and component wear. Åström and Hägglund (1995) note that switching between different control modes using split-range control can cause difficulties, including oscillations.

The control performance with the split-range sequencing strategy can be improved by using an adaptive controller to adjust the proportional gain and integral time of the PI controller. One such controller is described by Seem (1998). However, the control parameters may need significant adjustment as the control switches from one device to another. For example, the controller parameters may need to change significantly as the control goes from heating to cooling with outdoor air. During the time period that the adaptive controller is adjusting parameters in the transition region, the control performance will be sacrificed.

FINITE STATE MACHINE SEQUENCING CONTROL STRATEGY

Figure 4 shows a state transition diagram for implementing a FSM sequencing control strategy. The states shown in Figure 4 are described below.

State 1

In State 1, feedback control is used to modulate the flow of hot water to the heating coil, thereby controlling the amount of energy transferred to the air. Meanwhile, the mixing box dampers are positioned for the minimum outdoor air required for ventilation and the cooling coil valve is closed. The transition to State 2 occurs after the control signal has been saturated at the no heating position for a time period equal to the state transition delay.

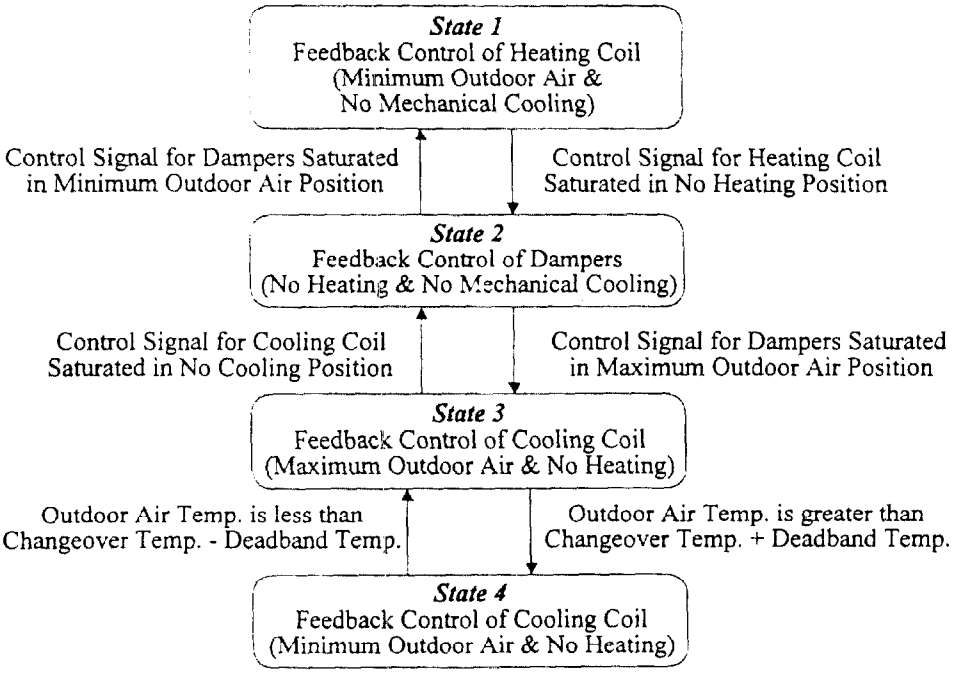

Figure 4. Finite state machine control strategy for air-handling units

State 2

In State 2, feedback control is used to adjust the position of the mixing box dampers in order to maintain the supply air temperature at the setpoint value. Adjusting the positions of the dampers varies the relative amounts of outdoor air and return air in the supply air stream. In State 2, the heating and cooling coil valves are closed. Transition to State 1 occurs after the control signal for the dampers has been at the minimum outdoor air position for a time period equal to the state transition delay. Transition to State 3 occurs after the control signal for the dampers has been at the maximum outdoor air position for a time period equal to the state transition delay.

State 3

In State 3, feedback control is used to modulate the flow of cold water to the cooling coil, thereby controlling the amount of energy extracted from the air. The outdoor air damper is set completely open and the heating coil valve is closed. Transition to State 2 occurs after the control signal for mechanical cooling has been saturated at the no cooling position for a time period equal to the state transition delay. Economizer logic is used to determine the transition to State 4. Either enthalpy based or temperature based economizer logic can be used. In the state transition diagram shown in Figure 4, logic based on outdoor air temperature is used to determine the transition point. Transition to State 4 occurs when the outdoor air temperature is greater than the changeover temperature plus the deadband temperature. Typically, the changeover temperature equals the return air temperature, and the deadband is about 0.56 °C. The purpose of the deadband temperature is to prevent cycling from State 3 to State 4 due to noise in the return and outdoor air temperature sensor readings.

State 4

State 4 also uses feedback control to modulate the flow of cold water to the cooling coil, thereby controlling the amount of energy extracted from the air. However, in this case, the outdoor air damper is set at the minimum outdoor air position. Economizer logic is used to determine the transition to State 3. In the state transition diagram shown in Figure 4, transition to State 3 occurs when the outdoor air temperature is less than the changeover temperature minus the deadband temperature.

Figures 3 and 4 illustrate the contrast in the paradigms of the split-range and the FSM control strategies. The paradigm shift consists of moving from continuous transitions between modes of control with split-range control, to discrete transitions with the FSM control. The state transition diagram provides a straightforward illustration of the discrete logic of the FSM control strategy. The improved clarity of the FSM control logic illustrated for this application becomes even more apparent and important as the complexity of the system operation increases. Auslander et al. (1996) discusses the use of state transition diagrams for designing digital control logic.

In this study, the FSM control strategy presented in Figure 4 is used to control the supply air temperature using three separate feedback controllers. One controller is dedicated to controlling the heating coil, one to the cooling coil, and one to the dampers. By using separate controllers for each process, the controller gains for each controller can be tuned to match the dynamic characteristics of the process it is controlling without regard for the other processes. At any given time, the FSM logic only allows one controller to be operating.

VALIDATION OF THE FINITE STATE MACHINE CONTROL STRATEGY

The first phase of the comparison of the FSM and split-range control strategies was a validation exercise. The purpose of this exercise was to ensure that the two strategies produce the same (or nearly the same) results when identical tuning parameters are used for both strategies and the state transition delay (used with the FSM control strategy) is set to zero. The procedures followed to determine the process and controller gains are described in the next two sections. The simulations

performed in this study used the building system simulation program HVACSIM+ (Park et al. 1985). The AHU model was built up from individual component models, including models for the supply and return air fans, the heating and cooling coils, valves, actuators, dampers, feedback controllers, and temperature sensors (Kohonen et al. 1993). The FSM and split-range control strategies were programmed as component models. Characteristics of the component models are provided in the appendix.

Process Parameters

A common method for tuning PI controllers is to assume the process to be controlled can be modeled as a first-order plus time-delay process (Seborg et al., 1989). Well known design relationships have been developed to compute the controller gains for processes that can be modeled in this way. The first-order plus time-delay model is given by

$$G(s) = \frac{Ke^{-\tau_d s}}{1 + s\tau} \tag{1}$$

where $G(s)$ is the transfer function for the process dynamics in the Laplace domain, K is the process gain, τ is the process time constant, and τ_d is the process delay time. The process parameters for the heating and cooling coil subsystems and the mixing box damper subsystem were determined from open-loop step tests in which the input to a valve or the dampers underwent a step change and the resultant dynamic response of the process variable was recorded. Seborg et al. (1989) describes several techniques for computing the unknown process parameters from the dynamic response to a step change in the input. In this study, non-linear regression techniques were used to determine the unknown process parameters.

The open-loop step test for the heating coil was performed with the outdoor air damper set at 10% open and the outdoor air temperature set at −16.1°C. The cooling coil was tested with the outdoor air damper set at 100% open and the outside air temperature set at 36.1°C. The open-loop step test of the mixing box dampers was performed with the outdoor and return air temperatures set at −16.1°C and 24°C, respectively. The conditions used for the step tests were selected because they were expected to yield the largest process gains that the various control loops would experience. The motivation for examining the regions of high process gain when determining the process parameters of the first-order plus delay time model will be more evident in the next section.

Steady-state responses of the heating and cooling coils at various valve positions showed that the largest changes in the process output to a step change in the input occurred when the valves were positioned between 0% and 40% open. This indicates that the process gain is largest in this range of valve positions. Thus, a step test in which the control signal to the heating coil valve was changed from 0% to 40% open (with the cooling coil valve closed) was performed to determine the heating coil process parameters. This test was then repeated for the cooling coil. Steady-state tests of the mixing box dampers indicated that the region of highest process gain corresponded to outdoor air damper positions ranging from 30% to 70% open. Thus, a step test was performed in which the control signal to the mixing box dampers were stepped from 30% to 70% of full scale. The process parameters obtained from the step tests are given in Table 1.

Table 1. Process Parameters Obtained from Step Tests

Process	K, °C^{-1}	τ, s	τ_d, s
Heating coil	39.3	75.0	65.2
Cooling coil	48.6	37.4	48.2
Mixing box dampers	63.7	75.9	70.9

Controller Parameters

With the process parameters of the first-order plus time-delay model known, the parameters for a PI control algorithm can be determined. A typical form of the PI algorithm is

$$u(t) = K_P\left(e(t) + \frac{1}{T_I}\int_0^t e(t^*)\,dt^*\right) \tag{2}$$

where $u(t)$ is the controller output at time t, K_P is the proportional gain, T_I is the integral time, $e(t)$ is the process error representing the deviation of the measured process output from a reference or setpoint value, and t^* is a dummy variable.

The control parameters for the heating and cooling coil control loops and the mixing box dampers control loop are calculated from relations obtained by minimizing a performance index for the integral of the time-weighted absolute error (ITAE) of a dynamic process subjected to a step change in load. The ITAE performance index is given by

$$\text{ITAE} = \int_0^\infty t^*\left|e(t^*)\right|\,dt^* \tag{3}$$

The relations used here come from Seborg et al. (1989) and were obtained assuming the process could be represented by a first-order plus time-delay model. The controller design relations for a PI controller subjected to a step change in load are

$$K_p = \frac{0.859}{K}\left(\frac{\tau_d}{\tau}\right)^{-0.977} \tag{4}$$

and

$$T_I = \frac{\tau}{0.674}\left(\frac{\tau_d}{\tau}\right)^{0.680} \tag{5}$$

The PI controller parameters for the heating coil, cooling coil, and mixing box dampers for the simulated system are given in Table 2. The parameters in Table 2 are referred to as optimal controller parameters because they result in a minimum value of the ITAE performance index for the given process parameters. In Table 2 and tables throughout the remainder of this paper, FSMCS refers to the FSM control strategy, and SRCS refers to the split-range control strategy.

The PI controller parameters for the FSM control strategy were obtained by direct substitution of values in Table 1 into Equations (4) and (5). The proportional gains for the split-range control strategy are one-third of those for the FSM strategy. This stems from the fact that each controller output is scaled so its output ranges from zero to unity. Since a single controller is used for the split-range strategy, and three controllers are used for the FSM strategy, the proportional gain for the split-range strategy must be scaled accordingly. Once the control mode is determined with the split-range strategy, the controller output is multiplied by a factor of three and shifted so that the input to the appropriate actuator ranges from zero to unity.

The controller parameter settings in Table 2 are representative of "well tuned" individual control loops for the three devices that are controlled. In this study, a number of other controller parameter settings are defined and compared for the split-range and FSM control strategies. The proportional gain for a "conservative" controller is defined as

$$K_{con} = \min\{K_{cc}, K_{hc}, K_{dm}\},$$

Table 2. Optimal Controller Parameters Based on Minimization of ITAE Performance Index

Controlled Component or Subsystem	K_P for FSMCS, °C^{-1}	K_P for SRCS, °C^{-1}	T_I, s
Heating Coil	0.0251	0.0084	101.13
Cooling Coil	0.0138	0.0046	65.89
Mixing Box Dampers	0.0144	0.0048	107.49

where K_{cc} is the proportional gain in Table 2 obtained by tuning the cooling coil, K_{hc} is the proportional gain obtained by tuning the heating coil, and K_{dm} is the proportional gain obtained by tuning the mixing box dampers. As noted previously, if a single PI controller is used to control all three devices, the controller should be tuned for the worst-case conditions to ensure stable control. The conservative controller accomplishes this goal. For this system, the conservative controller uses the proportional gain and integral time obtained by tuning the cooling coil (proportional gain obtained by tuning the cooling coil is the minimum of those in Table 2).

A "sluggish" controller is defined as a controller with a proportional gain equal to one-half the value of K_{con}, and a "very sluggish" controller is defined as a controller with a proportional gain equal to one-fifth the value of K_{con}. The integral time used for the "conservative" controller was also used for the sluggish and very sluggish controllers.

The proportional gain for a "responsive" controller is defined as

$$K_{res} = \max \{K_{cc}, K_{hc}, K_{dm}\},$$

where K_{cc}, K_{hc}, and K_{dm} are defined above. The responsive controller ignores the premise that the PI controller should be tuned for the worst-case conditions. For this system, the responsive controller used the proportional gain and integral time obtained by tuning the heating coil.

An "aggressive" controller is defined as a controller with a proportional gain equal to two times the value of K_{res}, and a "very aggressive" controller is defined as a controller with a proportional gain equal to five times the value of K_{res}. The integral time used for the responsive controller was also used for the aggressive and very aggressive controllers. Controller parameters corresponding to the six non-optimal cases are given in Table 3.

Artificial Outdoor Air Temperature Profile

The validation of the control strategies was performed using the artificial outdoor air temperature profile shown in Figure 5. As seen in Figure 5, a five-day profile was used and the range of the artificial outdoor air temperature profile was from –20°C to 40°C. This profile was

Table 3. Non-Optimal Controller Parameters

Control Case	K_P for FSMCS, °C^{-1}	K_P for SRCS, °C^{-1}	T_I, s
Very Sluggish Control	2.8×10^{-3}	9.33×10^{-4}	65.89
Sluggish Control	6.9×10^{-3}	2.3×10^{-3}	65.89
Conservative Control[1]	1.38×10^{-2}	4.6×10^{-3}	65.89
Responsive Control[2]	2.51×10^{-2}	8.367×10^{-3}	101.13
Aggressive Control	5.02×10^{-2}	1.667×10^{-2}	101.13
Very Aggressive Control	1.255×10^{-1}	4.183×10^{-2}	101.13

[1] Conservative control parameters correspond to cooling coil control parameters in Table 2.
[2] Responsive control parameters correspond to heating coil control parameters in Table 2.

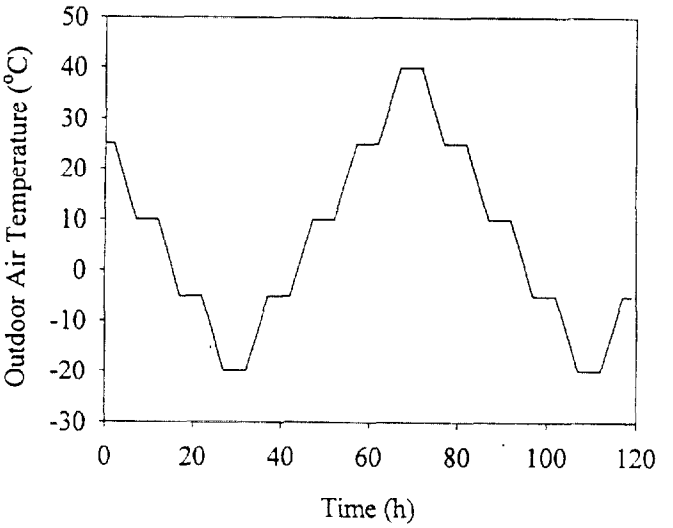

Figure 5. Outdoor air temperature profile for validation of the FSM control strategy

chosen because it was expected to force the system into all possible modes of AHU operation, and because the results were expected to be more tractable than results obtained with actual weather data.

Validation Results

To validate that the two control strategies yield nearly the same results when the state transition delay is zero, seven simulations were performed for each of the strategies. For each simulation, the same controller gains were used for the three devices that were controlled. Six of the simulations used the controller gains listed in Table 3. The seventh simulation used controller gains obtained by tuning the mixing-box dampers. In this study, the proportional gain for the mixing-box dampers falls between that for the heating coil (conservative control) and the cooling coil (responsive control).

For the validation simulations, a constant supply air temperature setpoint equal to 12.8°C and a constant return air temperature equal to 24°C were used in conjunction with the outdoor air temperature profile in Figure 5. The minimum outdoor air damper position was set at 10%. The supply airflow rate was maintained at a constant value. The state transition delay of the FSM control algorithm was set to zero. In other words, immediate switching from one state to another was allowed.

Table 4 shows the results of the validation simulations in terms of three performance indicators. In Table 4, SSR is the number of actuator starts, stops, and reversals, *TD* is the actuator travel distance, and AIAE is the average of the integrated absolute value of the supply air temperature error ($T_{set} - T$). The energy use of the fans and in the coils was nearly the same for the two strategies and, therefore, is not presented.

The simulation results were somewhat unstable during the initial hours of the simulation. To minimize the influence of the initial conditions, only the data for hours 30 to 110 were analyzed. The results in Table 4 demonstrate that the performance of the control strategies is very similar. This testing also demonstrated that the coding of the two algorithms was correct.

There are two main reasons why the two control strategies give slightly different results for this limiting case where the state time delay is zero. The first and most important reason is that the two strategies are inherently different. The split-range control strategy has a single control loop producing a single continuous control signal. The control of the three devices is determined

Table 4. Validation Results

Control Parameters	SSR		*TD*		AIAE, °C	
	SRCS	FSMCS	SRCS	FSMCS	SRCS	FSMCS
Very Sluggish	390	387	13.07	13.05	0.635	0.639
Sluggish	827	823	21.92	21.82	0.472	0.467
Conservative	1337	1339	32.30	32.39	0.356	0.352
Responsive	1748	1756	40.87	41.01	0.297	0.296
Aggressive	2635	2628	59.73	59.72	0.212	0.214
Very Aggressive	10707	10722	275.48	276.45	0.207	0.218
Damper	1214	1185	29.74	29.19	0.400	0.393

by the value of control signal relative to a single continuous scale. On the other hand, the FSM control strategy uses three separate control loops, each producing its own control signal. Each control loop has a separate integral term, whereas the split-range control strategy has a single integral term.

Machine precision is the second reason the two control strategies do not produce the same results for the validation exercises. Extensive numerical testing was performed in an effort to demonstrate that nearly identical results could be obtained from the two algorithms. This testing included modifications to the FSM algorithm such that a single control loop was used to determine the control signal to each device. This testing demonstrated that during the initial hour of a simulation, control signals identical to the sixth decimal place could be obtained from the two algorithms. However, over time the solutions would begin to drift apart to a small degree, thereby leading to the conclusion that machine precision was one limiting circumstance in the validation exercises.

COMPARISON OF SEQUENCING STRATEGIES

Selection of the State Transition Delay

The performance of the FSM control strategy is dependent on the selection of the state transition delay time. If the state transition delay is too long, control will tend to be sluggish. If the delay is too short, the performance of the FSM control strategy will approach that of the split-range control strategy and problems with cycling between modes of operation will be more common. Hence, it is expected that an optimum (or near-optimum) state transition delay exists that will lead to the best compromise between actuator use (reduced by using larger values of the state transition delay) and the supply air temperature error (likely to be reduced by using smaller values of the state transition delay) over a range of operating conditions.

Simulations using the five-day artificial weather profile shown in Figure 5 were performed to determine the appropriate value of the state transition delay for the considered system. The simulations used the very aggressive control parameters listed in Table 3 for each control loop. The combination of very aggressive control parameters and the artificial weather profile was chosen because they lead to highly oscillatory responses with the FSM control strategy when the state transition delay is zero. Thus, the influence of the value of the state transition delay should be evident from the system response. Because the initial hours of the simulation were very unstable, only hours 30 through 110 of the simulation results were considered in determining the state transition delay. This time period encompasses one complete cycle of the artificial outdoor air temperature profile from its minimum value to its maximum and back to its minimum.

For the simulations, the minimum outdoor damper position was set to 25%. A reset schedule was employed in the air-handling controller that adjusted the supply air temperature setpoint

and the return air temperature based on the outdoor air temperature. If the outdoor air temperature was less than 1.7°C, the supply air temperature setpoint was set at 29.4°C and the return air temperature was set at 18.3°C. If the outdoor air temperature was greater than 21.1°C, the supply air temperature setpoint was set at 12.8°C and the return air temperature was set at 23.8°C. For outdoor air temperatures between 1.7°C and 21.1°C, the supply air temperature setpoint and the return air temperature were varied linearly between their limiting values. This reset control schedule might be used for an AHU that serves perimeter zones with a single common exposure (i.e., only zones with a northern exposure). Of course, the terminal boxes would require controls sophisticated enough to reverse the action of the dampers depending upon whether heating or cooling was needed.

The results of the effect of the state transition delay on the performance of the FSM control strategy are given in Table 5. STD is the state transition delay time. E_{sf}, E_{rf}, E_{hc}, and E_{cc} are the energy use by the supply fan, return fan, heating coil, and cooling coil, respectively. SSR, *TD*, and AIAE retain their previous definitions. The results in Table 5 indicate that as the state transition delay time is increased, the total energy use and the actuator performance parameters (SSR and *TD*) decrease essentially monotonically to what appear to be asymptotic values. The error parameter (AIAE) actually increases slightly as STD is increased from 0 to 30 s and then to 60 s, before decreasing to a minimum value of 2.1°C and then increasing slightly to 2.2°C for STD = 900 s.

The results in Table 5 indicate that for this system and the given weather profile, the performance parameters are insensitive to the state transition delay time as long as it is at least 180 s. However, a comparison of the supply air temperature responses for STD = 300 s and STD = 900 s reveals a degradation in the performance of the FSM control strategy for the larger delay time. Figures 6a and 7a show the control signals for the dampers, heating coil valve, and cooling coil valve for STD = 300 s and 900 s, respectively. Both figures show the FSM control strategy transitioning at $t \approx 85$ h from mechanical cooling with maximum outdoor air (State 3 in Figure 4) to cooling with outdoor air and no heating or mechanical cooling (State 2 in Figure 4). Figures 6b (STD = 300 s) and 7b (STD = 900 s) show that the larger value of the state transition delay leads to a significantly larger error between the supply air temperature and its setpoint value at this transition point. The obvious short-term difference in performance of the control strategy seen in Figures 6 and 7 is obscured in the results in Table 5 by the fact that only a small number of state transitions occur in the 80 h of simulation data that were used to compile the results. A second index that identified the worst-case error could also be used to determine the appropriate value of the state transition delay.

The effect of the value of the state transition delay on the performance of the FSM control strategy was also examined for realistic weather data profiles for the months of January and April. Specifically, three actual weather days of data from the "Weather Year for Energy Calculation" (WYEC) tape were selected that were deemed to be representative of the data for an entire month.

Table 5. Dffect of State Transition Delay on Performance of FSM Control Strategy Using Artificial Outdoor Air Temperature Profile

STD, s	SSR	*TD*	E_{sf}, kJ	E_{rf}, kJ	E_{hc}, kJ	E_{cc}, kJ	AIAE, °C
0	8258	4198	1086.0	199.5	15458	10389	6.5
30	6328	3484	1086.0	199.5	11103	6716	9.2
60	5746	2834	1086.0	199.5	8846	5110	9.8
180	3839	779	1086.0	199.5	8042	4254	2.1
300	3813	777	1086.0	199.5	7994	4255	2.1
600	3784	775	1086.0	199.5	7955	4254	2.1
900	3760	777	1086.0	199.5	7998	4249	2.2

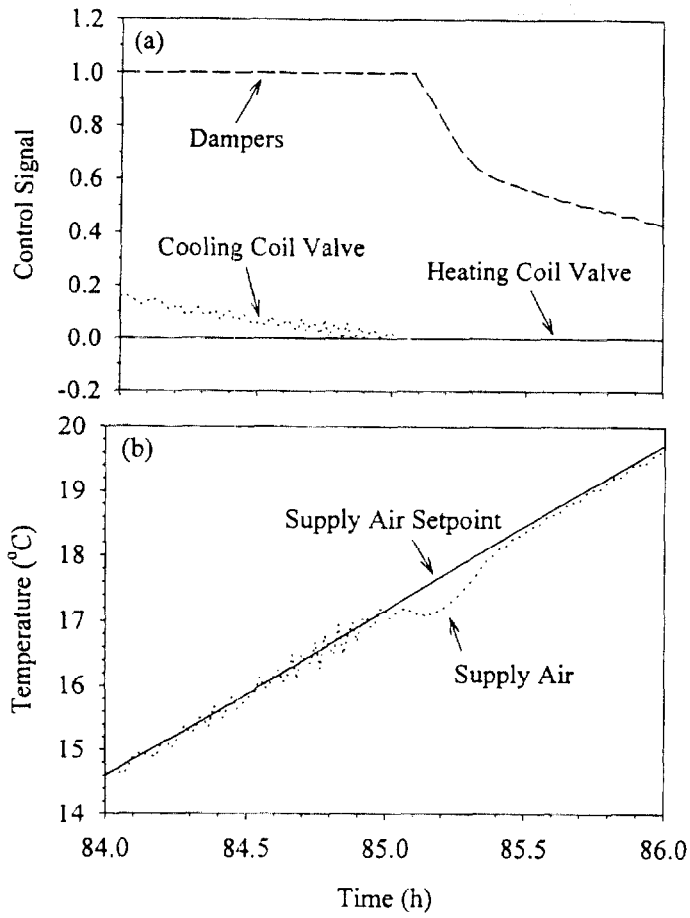

Figure 6. Supply air temperature response to a state transition for STD = 300 s

The methodology described by Nall et al. (1981) was used to abbreviate the weather data. The January weather data for Salt Lake City is plotted in Figure 8 along with several other abbreviated monthly weather data profiles. The April weather data profile is not shown in Figure 8; however, March and May profiles are shown and the April profile falls between the profiles of those months. January and April weather data were selected because, when the value of the state transition delay is zero, this weather data coupled with improper tuning of the controllers results in highly oscillatory responses for the FSM control strategy. That is, these conditions lead to a worst-case scenario in terms of the performance of the controllers.

The results for the realistic weather data profile for January are shown in Table 6. The same trends observed in Table 5 are seen in Table 6 and also in the April data that is not presented. That is, based on the cumulative measures in Table 6, there is very little difference in the performance of the FSM control strategy for state transition delay times of 180 s or greater. It should be noted that the negative values of E_{cc} in Table 6 are due to numerical precision problems cited previously.

It is difficult to generalize the results in Tables 5 and 6 other than to state that the selection of the appropriate state transition delay for a given system will likely require a certain amount of engineering judgment and perhaps some trial and error tuning. A state transition delay time of three to five minutes would seem to be a reasonable value that will decrease cycling between

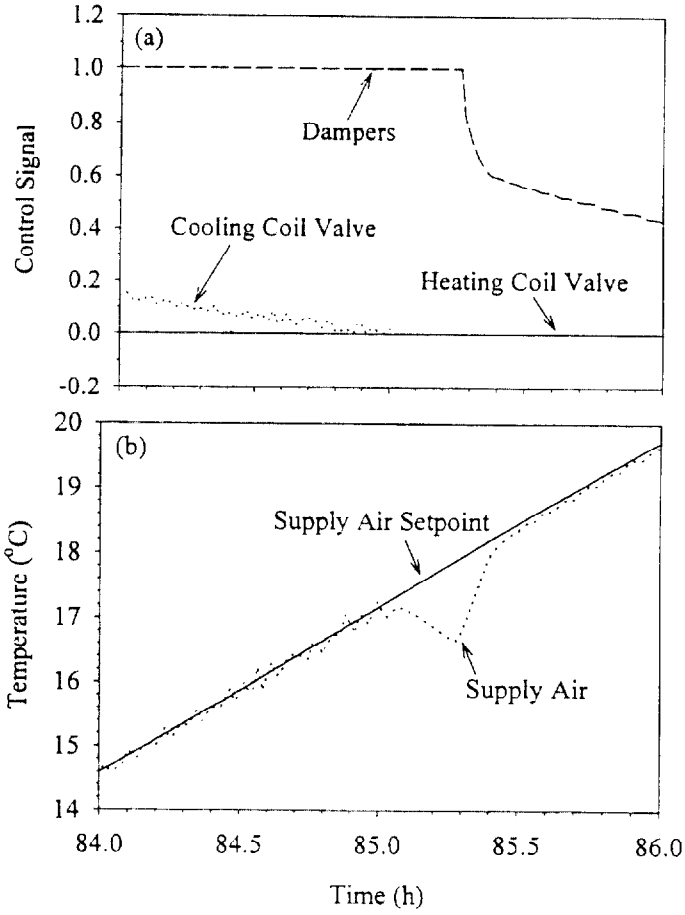

Figure 7. Supply air temperature response to a state transition for STD = 900 s

Table 6. Effect of State Transition Delay on Performance of FSM Control Strategy Using January Weather Data Profile

STD, s	SSR	*TD*	E_{sf}, kJ	E_{rf}, kJ	E_{hc}, kJ	E_{cc}, kJ	AIAE, °C
0	5263	3283	732.2	195.1	10280	4205	11.2
30	3944	2666	732.2	195.1	7589	1600	14.7
60	3402	2161	732.2	195.1	5939	523	15.4
180	2252	520	732.2	195.1	4334	−3	2.5
300	2254	520	732.2	195.1	4328	−6	2.5
600	2237	521	732.2	195.1	4334	−3	2.5
900	2251	521	732.1	195.1	4333	−5	2.5

modes of operation without substantially affecting the capability of the system to maintain the supply air temperature at the setpoint value. In the results presented in the next section, a state transition delay time of five minutes was used.

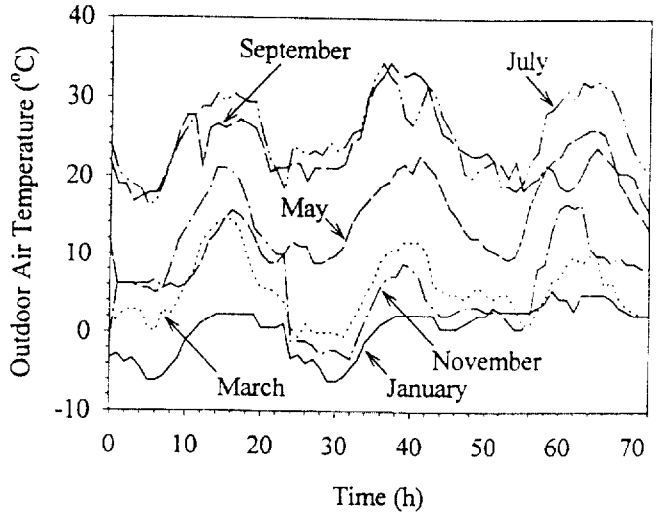

Figure 8. Three-day outdoor air temperature profiles for various months in Salt Lake City, Utah

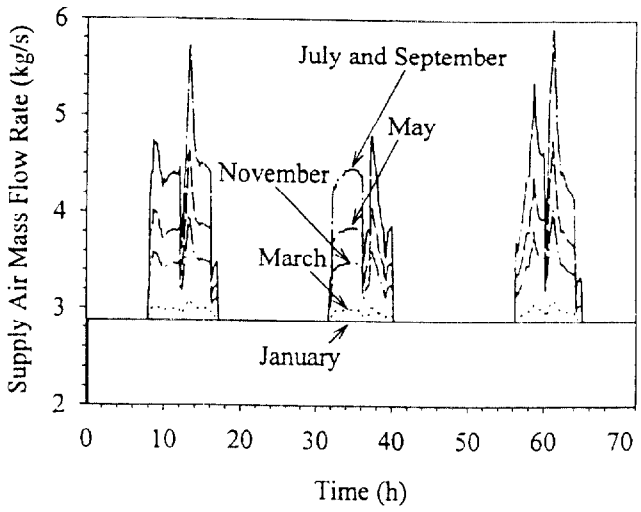

Figure 9. Three-day supply airflow rate profiles for various months

Yearly Simulation Conditions

A proper assessment of the performance of the two sequencing control strategies can only be achieved through long-term comparisons. To this end, simulations were run using representative three-day weather data profiles (selected from the WYEC tape) for each month of the year for Salt Lake City. Three-day outdoor air temperature profiles are plotted in Figure 8 for selected months.

The reset schedule described in the previous section was used to establish the supply air temperature setpoint. To simulate a variable-air-volume system, the supply airflow rate was varied according to the three-day profiles shown for select months in Figure 9. The return airflow rates

were set at 90% of the supply airflow rates. The supply airflow profile for a month not shown in Figure 9 falls between the profiles of its neighbors.

The supply and return air fans operated continuously. During unoccupied periods, the supply airflow rate was set at the minimum value shown in Figure 9 (approximately 2.9 kg/s). The minimum damper position was set to 25% to increase the influence of the outdoor air temperature on system operation. The dry-bulb economizer deadband was set to 0.56°C and the changeover temperature was set to 20°C. For all actuators, the traveling time between the position limits was set to 200 s, and the deadband of the actuators was set to 2% of the travel distance between the limits.

Yearly Simulation Results

Figure 10 shows four hours of the January simulation results for the split-range control strategy using very aggressive controller parameters. The data presented is representative of the entire data set for the January conditions. In addition, by limiting the amount of data presented, it is possible to gain an understanding of the operation of the system that cannot be achieved by examining a plot of the entire January data set. The supply air temperature and setpoint, outdoor air temperature, mixed air temperature, and return air temperature are plotted in Figure 10a. The supply and outdoor air mass flow rates are plotted in Figure 10b. The control signals for the dampers, the heating coil valve, and the cooling coil valve are plotted in Figure 10c.

The results in Figure 10 demonstrate the type of unstable control that can occur in systems controlled using split-range control. In particular, the control signals in Figure 10c show that the dampers and heating coil valve are alternately oscillating between their minimum and maximum values in an attempt to control the supply air temperature. Because the control parameters are too aggressive, the dampers open too much, allowing too much cold, outdoor air into the mixing plenum. This causes the mixed air temperature to be too cold, which leads to the supply air temperature being below the setpoint value. The dampers then close and the heating coil valve opens in order to bring the supply air temperature back to the setpoint. However, the aggressiveness of the heating coil valve causes the supply air temperature to increase to a value greater than the setpoint, thereby starting the process over again.

Four hours of the January simulation results are shown in Figure 11 for the FSM control strategy using very aggressive controller parameters for each control loop. The state transition time was set to 300 seconds. The results in Figure 11a show that the supply air temperature is still very unstable, however, the mixed air temperature does not oscillate as it did for the split-range control strategy. The control signals in Figure 11c show that the heating coil control is also very unstable, but that the damper control signal is no longer oscillating. The results for the FSM control strategy clearly represent an improvement over those for the split-range control strategy.

Because the FSM control strategy has three separate controllers, it is possible to use different controller parameters in each. Four hours of the January simulation results are shown in Figure 12 for the FSM strategy using optimally tuned controller parameters determined independently for each control loop. The optimally tuned controller parameters are given in Table 2 for the three controllers (heating coil, cooling coil, and dampers). The results in Figure 12 show that the system operation is stable when the optimally tuned controller parameters for each control loop are used.

Yearly simulation results are summarized in Table 7. The results in Table 7 indicate that, unless the controllers are tuned too aggressively, there is little difference in the two strategies from the standpoint of actuator use, supply air temperature error and energy use. However, for systems in which the controllers are tuned too aggressively, the differences in these parameters are quite large. For the very aggressive case, the energy use in the heating coil and the cooling coil are 31% and 13% less for the FSM control strategy in comparison to the split-range control strategy. In addition, Table 7 shows that the FSM control strategy reduces the number of starts, stops, and reversals of the actuators by 58% and reduces the actuator travel distance by 79%. Finally, the

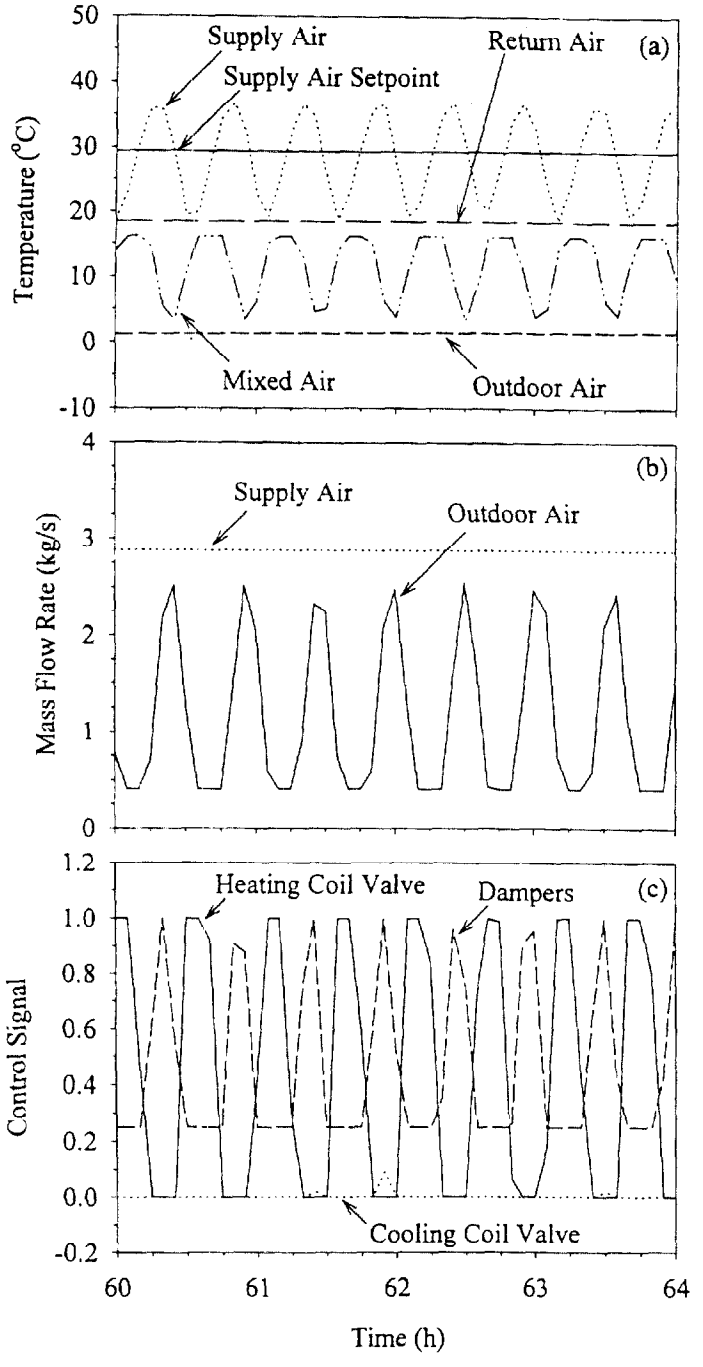

Figure 10. Split-range control strategy results for January weather data using very aggressive control parameters

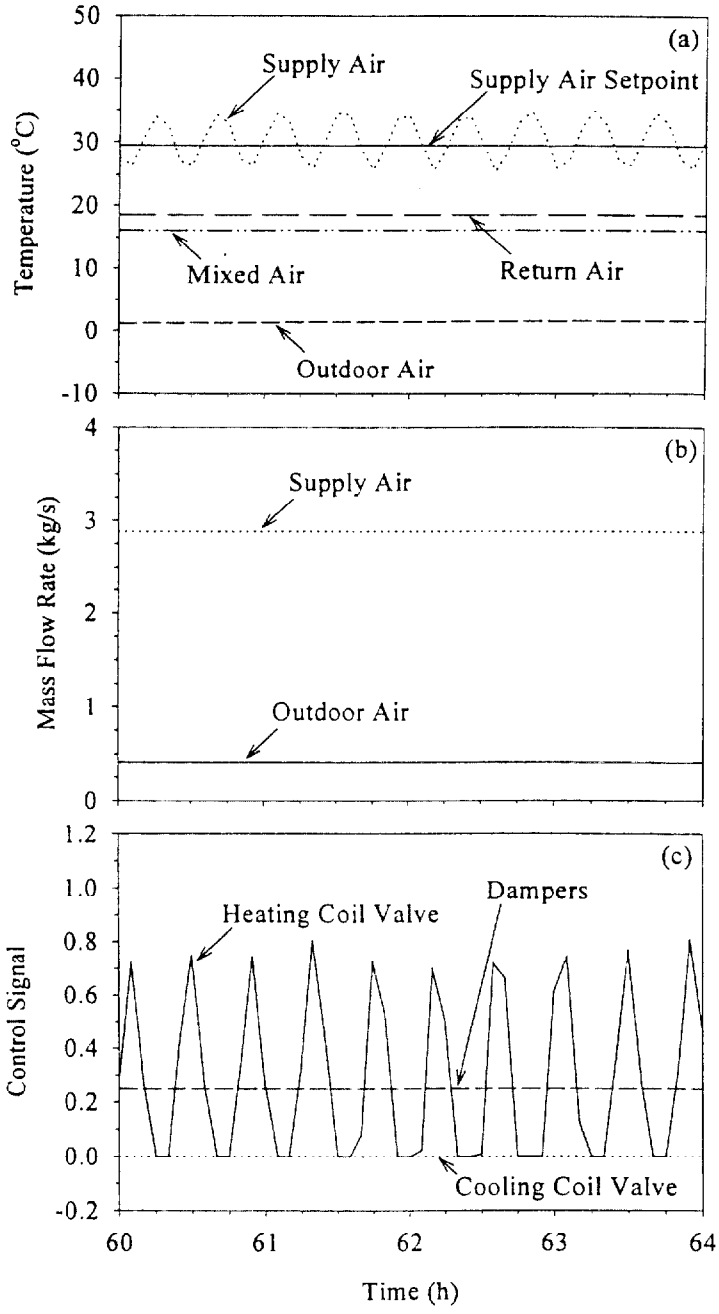

Figure 11. FSM control strategy results for January weather data using very aggressive control parameters

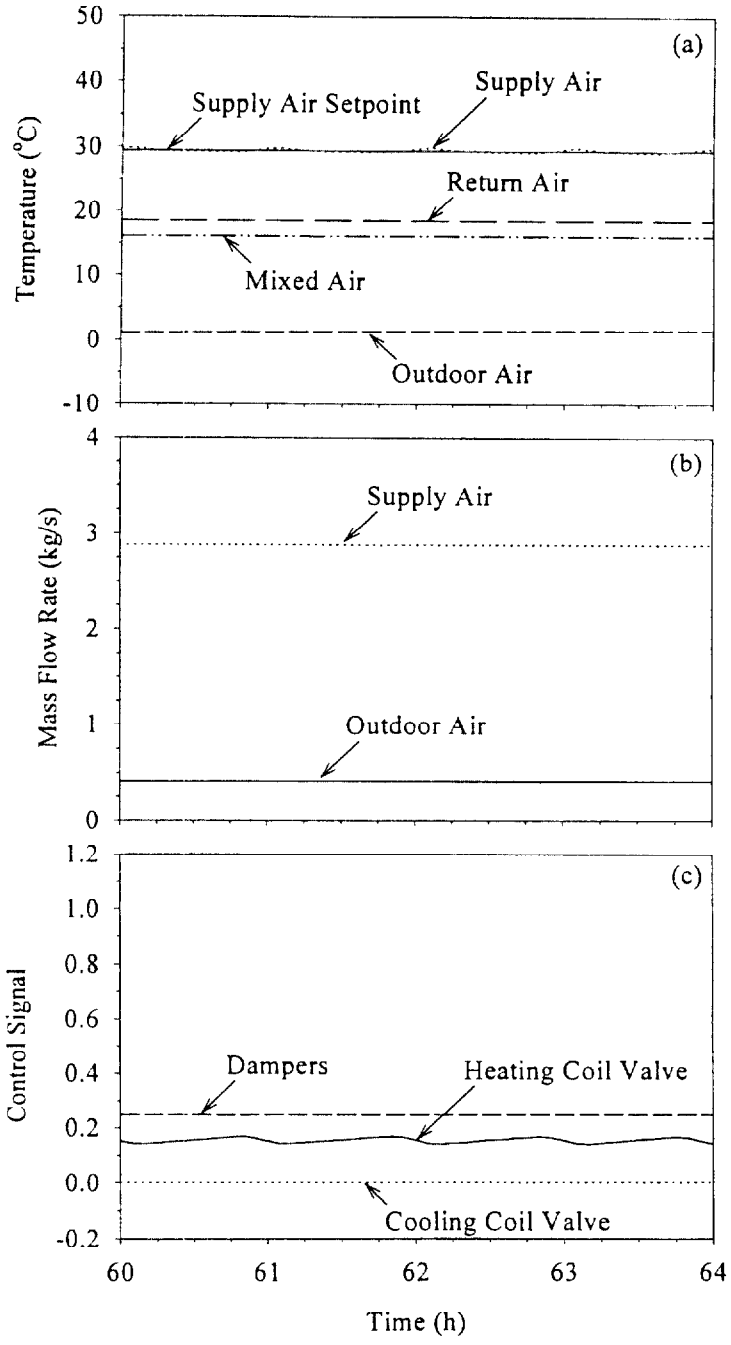

Figure 12. FSM control strategy results for January weather data using optimally tuned control parameters

Table 7. Summary of Yearly Simulation Results

(a) Actuator Use and Supply Air Temperature Error

	SSR		*TD*		AIAE, °C	
Control Parameters	**SRCS**	**FSMCS**	**SRCS**	**FSMCS**	**SRCS**	**FSMCS**
Very Sluggish	2984	3009	91.6	92.8	0.95	0.97
Sluggish	4334	4351	118.6	118.2	0.62	0.63
Conservative	5857	6100	147.2	152.8	0.47	0.51
Responsive	7505	7485	179.7	180.6	0.41	0.43
Aggressive	21463	19256	499.5	454.6	0.43	0.44
Very Aggressive	46620	19767	16549.7	3540.3	4.32	1.88
Damper	5347	5338	137.6	138.2	0.53	0.55
Optimally Tuned		7366		177.0		0.48

(b) Energy Use

	E_{hc}, kJ		E_{cc}, kJ	
Control Parameters	**SRCS**	**FSMCS**	**SRCS**	**FSMCS**
Very Sluggish	29274	29258	37109	37092
Sluggish	29266	29264	37388	37371
Conservative	29027	29280	37440	37428
Responsive	29274	29272	37441	37435
Aggressive	29218	29253	37452	37449
Very Aggressive	46745	32158	43104	37462
Damper	29227	29283	37413	37403
Optimally Tuned		29271		37408

AIAE is 56% less for the FSM control strategy, indicating that the control of the supply air temperature is significantly improved.

From Table 7 it can seen that the results for the optimally tuned control parameters fall between the conservative and responsive results. In particular, as the control parameters become more responsive (i.e., as the proportional gain increases), the parameters quantifying actuator use (SSR and *TD*) increase, while the value of the AIEA decreases. However, the differences in these performance measures are not large when one considers only conservative, optimal, and responsive control parameters. These differences would be expected to be more substantial if the process dynamics of the three control loops showed more variation. For instance, in many cases the process dynamics of the heating coil and the cooling coil are considerably different. In such a case, the flexibility provided by the three separate control loops of the FSM control strategy would likely lead to a vast improvement in the control of the system compared to the split-range control strategy.

The results indicate that the benefits of the FSM control strategy are observed when the PI controller in the split-range control strategy is poorly tuned. This, however, is a common occurrence in the field (Seem 1998, ASHRAE 1995). The FSM control strategy can lessen the adverse effects of an aggressively tuned controller without negatively impacting the control of a system that is properly tuned. Finally, the FSM control strategy is straightforward to implement and the transition of the system from one control mode to another is tractable, in part because of the accompanying state transition diagram.

CONCLUSIONS

The objective of this paper was to introduce the finite state machine sequencing control strategy for AHUs and to compare this strategy with a traditional split-range sequencing control strategy. Simulation results obtained from representative weather data for each month of the year were presented to demonstrate the performance of the two sequencing strategies with respect to the controller gains (proportional gain and integral time) used for the heating coil, cooling coil, and mixing box dampers. The two strategies were found to perform nearly the same under most circumstances. However, when the PI controller was tuned too aggressively, the FSM control strategy yielded a 31% reduction in heating coil energy, a 13% reduction in cooling coil energy, improved temperature control, and reduced actuator use in comparison to the split-range control strategy.

The FSM control strategy represents a paradigm shift in the way sequencing logic is developed, illustrated, and implemented for the control of HVAC systems. The state transition diagram presents the logic in a manner that is straightforward to understand. The state transition delay helps alleviate instabilities caused by poor tuning. The use of separate PI controllers for each controlled process allows each controller to be tuned for the static and dynamic characteristics of a particular process. In contrast, the logic of the split-range control strategy is tied to the limitations of traditional pneumatic control systems. The logic is more difficult to understand and more difficult to implement. In addition, the typical approach of using a single PI controller to control multiple processes can lead to tuning difficulties and performance problems. The arguments made in favor of the FSM control strategy become even more apparent as the complexity of the control problem increases.

ACKNOWLEDGMENTS

This research was partially supported by the Office of Energy Efficiency and Renewable Energy, U. S. Department of Energy. The authors would like to acknowledge Dr. George E. Kelly, Group Leader of the Mechanical Systems and Controls Group at the National Institute of Standards and Technology, for his contribution to this study.

NOMENCLATURE

AIAE	average of the integrated absolute value of the error, °C
$e(t)$	error signal (e.g., $T_{set} - T$)
E_{cc}	cooling coil energy, kJ
E_{hc}	heating coil energy, kJ
E_{rf}	return fan energy, kJ
E_{sf}	supply fan energy, kJ
FSM	finite state machine
FSMCS	acronym for the finite state machine control strategy
$G(s)$	transfer function in the Laplace domain
K	process gain
K_{cc}	proportional gain computed using the process dynamics of the cooling coil loop and the ITAE design relations, $°C^{-1}$
K_{con}	conservative proportional gain, $°C^{-1}$
K_{dm}	proportional gain computed using the process dynamics of the mixing box dampers and the ITAE design relations, $°C^{-1}$
K_{hc}	proportional gain computed using the process dynamics of the heating coil loop and the ITAE design relations, $°C^{-1}$
K_P	proportional gain, $°C^{-1}$
K_{res}	responsive proportional gain, $°C^{-1}$
s	Laplace variable
SRCS	acronym for the split-range control strategy
SSR	number of starts, stops, and reversals of the actuator
STD	state transition delay, s
t	time, s
T_I	integral time, s
TD	travel distance of the actuator
$u(t)$	control signal
u_d	damper control signal
τ	process time constant, s
τ_d	process time delay, s

REFERENCES

Åström, K.J., and T. Hägglund. 1995. *PID Controllers: Theory, Design, and Tuning*, 2nd Ed. Instrument Society of America. p. 292.

ASHRAE. 1995. Building Operating Dynamics and Strategies. In 1995 *ASHRAE Handbook—HVAC Applications*, pp. 38.4-38.5. Atlanta: ASHRAE.

Auslander, D.M., J.R. Ridgely, and J.C. Jones. 1996. Real-Time Software for Implementation of Feedback Control. *The Control Handbook*. Chapter 17, Editor William S. Levine, CRC and IEEE Press.

Dickson, D.K., and S.T. Tom. 1986. Economizer Control Systems. *ASHRAE Journal* 28(9): 32-36.

Hartman, T.B. 1993. *Direct Digital Controls for HVAC Systems*. New York: McGraw-Hill.

Kohonen, R., S. Kärki, J. Hyvärinen, S. Wang, P. Nusgens, P. Haves, H.C. Peitsman, G.E. Kelly, J-C. Visier, H. Vaezi-Nejad, M. Jandon and C. Henry. 1993. *Synthesis Report: Development of Emulation Methods*. Espoo, Finland: VTT.

Nall, D.H., E.A. Arens, and L.E. Flynn. 1981. Abbreviation of Climate Data for Building Thermal Analysis Programs Using Representative Samples of Various Lengths. *ASHRAE Transactions* 87(1): 923-934.

Ogunnaike, B.A. and W.H. Ray. 1994. *Process Dynamics, Modeling, and Control*. Oxford University Press. p. 583.

Park, C., G.E. Kelly, and J.Y. Kao. 1984. Economizer Algorithms for Energy Management and Control Systems. U.S. National Bureau of Standards Publication. Gaithersburg, MD: National Institute of Standards and Technology.

Park, C., D.R. Clark, and G.E. Kelly. 1985. An Overview of HVACSIM+, a Dynamic Building/HVAC/Control System Simulation Program. *Proceedings of 1st Annual Building Energy Simulation Conference*. Seattle.

Seborg, D.E., T.F. Edgar, and D.A. Mellichamp. 1989. *Process Dynamics and Control*. New York: John Wiley & Sons.

Seem, J.E. 1998. A New Pattern Recognition Adaptive Controller with Application to HVAC Systems. *AUTOMATICA* 34(8): 969-982.

Spitler, J.D., D.C. Hittle, D.L. Johnson, and C.O. Pedersen. 1987. A Comparative Study of the Performance of Temperature-Based and Enthalpy-Based Economy Cycles. *ASHRAE Transactions* 93(2): 13-22.

Wang, S.K. 1993. *Handbook of Air Conditioning and Refrigeration*. New York: McGraw-Hill.

APPENDIX: SELECTED CHARACTERISTICS OF AHU COMPONENTS

The AHU model was built up from individual component models. Details of the component models can be found in Kohonen et al. (1993). Selected characteristics of the component models are provided below.

Actuators for Dampers and Valves

Actuator starting point	closed
Actuator travel time (limit to limit)	200 s
Deadband	0.02

Mixing Box

Outdoor air damper	opposed
Recirculation air damper	opposed
Exhaust air damper	opposed
Open resistance for outdoor air damper	1.27 E−04 pressure differential (kPa) at 1 m^3/s
Open resistance for recirculation air damper	2.23 E−04 pressure differential (kPa) at 1 m^3/s
Open resistance for exhaust air damper	2.23 E−04 pressure differential (kPa) at 1 m^3/s
Leakage for outdoor air damper	1.00 E+00 %
Leakage for recirculation air damper	1.00 E+00 %
Leakage for exhaust air damper	1.00 E+00 %

Authority of outdoor air damper	0.109
Authority of recirculation air damper	0.129
Authority of exhaust air damper	0.07

Heating Coil

Number of rows of tubes	1
Number of tubes per row	48
Number of parallel water circuits	6
Length of finned section in flow direction	3.80 E–02 m
Height of finned section	1.44 m
Width of finned section	1.36 m
Tube outside diameter	1.27 E–02 m
Tube wall thickness	4.30 E–04 m
Tube material	Copper
Fin spacing (pitch)	2.50 E+01 m
Fin thickness	1.60 E–04 m
Fin material	Aluminum
Flow resistance parameter on the air side	3.28 E–04 $(g \cdot m)^{-1}$
Coil hydraulic resistance	32.37 $(g \cdot m)^{-1}$

Cooling Coil

Number of rows of tubes	6
Number of tubes per row	45
Number of parallel water circuits	45
Length of finned section in flow direction	1.92 E–01 m
Height of finned section	1.44 m
Width of finned section	1.36 m
Tube outside diameter	1.27 E–02 m
Tube wall thickness	4.30 E–04 m
Tube material	Copper
Fin spacing (pitch)	2.10 E–03 m
Fin thickness	1.40 E–04 m
Fin material	Aluminum
Flow resistance parameter on air side	4.86 E–03 $(g \cdot m)^{-1}$
Coil hydraulic resistance	0.522 $(g \cdot m)^{-1}$

Heating Coil Valve

Valve mode	Exponential/Linear
Valve leakage	0.02 %

Cooling Coil Valve

Valve mode	Exponential/Linear
Valve leakage	0.02 %

Supply Fan

Diameter	0.57 m
Highest normalized flow	1.5
1st pressure coefficient	4.47318
2nd pressure coefficient	−1.30791
3rd pressure coefficient	6.16939
4th pressure coefficient	−5.75617
5th pressure coefficient	0.505184

Return Fan

Diameter	0.519 m
Highest normalized flow	1.5
1st pressure coefficient	4.47318
2nd pressure coefficient	−1.30791
3rd pressure coefficient	6.16939
4th pressure coefficient	−5.75617
5th pressure coefficient	0.505184